

From Supramolecular to Solid State Chemistry: Crystal Engineering of Luminescent Materials by Trapping Molecular Clusters in an Aluminium-based Host Matrix

Clément Falaise,^{*a} Anton A. Ivanov,^{a,b} Yann Molard,^c Maria Amela Cortes,^c Michael A. Shestopalov,^b
Mohamed Haouas,^a Emmanuel Cadot^a and Stéphane Cordier^{*c}

- a. Institut Lavoisier de Versailles, UMR 8180 CNRS, UVSQ, Université Paris-Saclay, Versailles, France.
- b. Nikolaev Institute of Inorganic Chemistry SB RAS, Novosibirsk, 630090, Russia.
- c. Institut des Sciences Chimiques de Rennes, UMR 6226 CNRS, Université de Rennes 1, Rennes, France

Table of contents

1. Experimental Procedures	3
a) General methods	3
b) Synthetic methods.....	5
i. Preparation of water-soluble salts of $\{[\text{Mo}_6\text{X}_i\text{Cl}_6^a]@2\text{CD}\}^{2-}$	5
ii. Preparation of the compounds built from $\{[\text{Mo}_6\text{X}_i\text{Cl}_6^a]@2\text{CD}\}^{2-}$	6
iii. Preparation of the compounds built from $\{\text{Mo}_6\text{X}_i\text{Cl}_6^a@2\text{CD}\}^{2-}$ and $\{\text{Al}_{13}\}^{7+}$	6
2. Single-crystal X-ray diffraction.....	8
a) Crystallographic parameters for 1-Br and 1-I (<i>table 1</i>).....	8
b) Crystallographic parameters for 2-Br and 2-I (<i>table 2</i>).....	9
c) Crystallographic parameters for 3-Br and 3-I (<i>table 3</i>).....	10
d) Crystallographic parameters of molecular clusters observed in the compounds 1-Br, 1-I, 2-Br, 2-I, 3-Br and 3-I (<i>tables 4-6 ; figures 1-3</i>).....	11
a) Views of the disordered clusters $[\text{Mo}_6\text{I}_6\text{Cl}_6]^{2-}$ in 2-I and 3-I (<i>figures 4-5</i>)	13
b) Views of the packing in the compounds 1-X and 2-X (<i>figures 6-7</i>)	14
c) Illustration of voids in the crystal structures (<i>figures 8-10</i>).....	15
3. ^1H NMR investigation	18
a) ^1H NMR titration of CD by $[\text{Mo}_6\text{Br}_8\text{Cl}_6]^{2-}$ (<i>figures 11-12</i>).....	18
b) ^1H NMR titration of CD by $[\text{Mo}_6\text{I}_8\text{Cl}_6]^{2-}$ (<i>figures 13-14</i>)	19
c) ^1H NMR titration of CD by $\{\text{Al}_{13}\}^{7+}$ (<i>figure 15</i>)	20
4. Electrospray ionization mass spectroscopy (ESI-Mass) (<i>figures 16-17</i>).....	21
5. Cyclic voltammetry experiments of the $[\text{Mo}_6\text{I}_8\text{Cl}_6]^{2-}$ /CD system in aqueous solution	22
a) Dependence of the peak currents upon potential scan rate (<i>figures 18-19</i>)	22
b) Cyclic voltammetry of $[\text{Mo}_6\text{I}_8\text{Cl}_6]^{2-}$ at different concentration of CD (<i>figures 20</i>).....	23
6. Photo-physical investigations.....	24
a) Solid state Excitation Map of compounds 1-I, 2-I and 3-I (<i>figures 21-23</i>)	24
b) Comparison of normalized emission spectra recorded in the solid-state (<i>figure 24</i>)	25
c) Time resolved photoluminescence mapping of compounds 1-I, 2-I and 3-I (<i>figure 25-30</i>)	25
7. Thermogravimetric analysis (<i>figure 31</i>).....	29
8. Reference	30

1. Experimental Procedures

a) General methods

Single-crystal X-ray diffraction. Crystals of **1-Br**, **1-I**, **2-Br**, **2-I**, **3-Br** and **3-I** were selected under polarizing optical microscope and glued in paratone oil to prevent any loss of crystallization water. X-ray intensity data were collected at low temperature ($T = 200(2)$ K) on a Bruker D8 VENTURE diffractometer equipped with a PHOTON 100 CMOS bidimensional detector using a high brilliance μS microfocus X-ray Mo $K\alpha$ monochromatized radiation ($\lambda = 0.71073$ Å). Data reduction was accomplished using SAINT V7.53a. The substantial redundancy in data allowed a semi-empirical absorption correction (SADABS V2.10) to be applied, on the basis of multiple measurements of equivalent reflections. Using Olex²¹, the structure was solved with the ShelXT² structure solution program using Intrinsic Phasing and refined with the ShelXL³ refinement package using Least Squares minimization. The remaining non-hydrogen atoms were located from Fourier differences and were refined with anisotropic thermal parameters. Positions of the hydrogen atoms belonging to the gamma-cyclodextrins were calculated and refined isotropically using the gliding mode. Crystallographic data for single-crystal X-ray diffraction studies are summarized in Table S1, S2 and S3 (see below). These data can be obtained free of charge from The Cambridge Crystallographic Data Centre via <https://www.ccdc.cam.ac.uk/structures-beta/>.

Deposit number: 1987553 for **1-Br**, 1987552 for **1-I**, 1987554 for **2-Br**, 1987556 for **2-I**, 1987555 for **3-Br** and 1987557 for **3-I**.

*Comments about the refinement of **1-Br** and **1-I**:* Due to the adding of NaCl in the reaction mixtures, extra Na^+ and Cl^- (3 NaCl per clusters; determined by EDX analysis) as well as water molecules located between the tubular arrangement are disordered. Most of the Na^+ and Cl^- have been located. No squeeze is requested for the refinement of these crystal structures. Using the option “Calc Solv” implemented in PLATON (calculation done considering the host-guest complexes, and the Na^+ and Cl^-), we determined that around 15% of the unit cell volume is accessible for water molecules.

*Comments about the refinement of **2-Br** and **2-I**:* The crystal structures reveal the presence of large voids which contain water molecules (H_2O) and counter cations disordered. Only few of them can be located using crystallographic data. Thereby the contribution of solvent-electron density was removed using the SQUEEZE routine in PLATON, producing a set of solvent-free diffraction intensities. Using the option “Calc Solv” implemented in PLATON (calculation done considering the host-guest complexes), we determined about 45% of the unit cell volume is accessible for water molecules. The crystal structure refinement of **2-I** reveals the cluster is disordered on two positions (50% occupancy).

*Comments about the refinement of **3-Br** and **3-I**:* As for the compound **2-I**, the structure refinement of **3-I** reveals that the cluster $\text{Mo}_6\text{I}_8\text{Cl}_6^{2-}$ is disordered on two positions (50% occupancy). In the compounds **3-Br** and **3-I**, the charge balancing is insured by 5 Cl^- anions per aluminum polycations $\{\text{Al}_{13}\}^{7+}$; four of them have been clearly located (around $\{\text{Al}_{13}\}^{7+}$; distance $\{\text{Al}_{13}\}^{7+}\cdots\text{Cl}$ is about 3.2 Å) defining a super-tetrahedron; the position of the remaining Cl^- was not identified. Thereby the contribution of solvent-electron density was removed using the SQUEEZE routine in PLATON, producing a set of solvent-free diffraction intensities. Using the option “Calc Solv” implemented in

PLATON (calculation done considering the host-guest complex, $\{Al_{13}\}^{7+}$, and 4 Cl^-), we determined about 41% of the unit cell volume is accessible for water molecules.

Photophysical measurements on powdered samples. Solid state emission vs excitation map and absolute quantum yield measurements were recorded using a hamamatsu C9920-02 set up made of a Xenon lamp, a monochromator, an integrating sphere equipped with a gas inlet and a PMA12 photodetector. Lifetime measurements and TRPL mapping were realized using a picosecond laser diode (Jobin Yvon deltadiode, 375 nm) and a Hamamatsu C10910-25 streak camera mounted with a slow single sweep unit. Signals were integrated on a 30 nm bandwidth. Fits were obtained using origin software and the goodness of fit is judged by the reduced χ^2 value and residual plot shape.

NMR studies. All NMR spectra were measured in D_2O at 27 °C. 1H NMR spectra have been collected using a Bruker Avance 400 spectrometer. Chemical shifts are reported relative to TMS for 1H according to conventions for standards.

Electrospray Ionization Mass Spectrometry (ESI-MS). Electrospray ionization mass spectra were collected using a Q-TOF instrument supplied by WATERS. Samples were solubilized in water at a concentration of 2.10^{-5} M and were introduced into the MS via an ACQUITY UPLC WATERS system whilst a Leucine Enkephalin solution was co-injected via a micro pump as internal standard.

Thermal gravimetric analysis. Water were determined by TGA with a Mettler Toledo TGA/DSC 1, STARE System apparatus or with a NETZSCH TG 209 F1 device under oxygen flow (50 mL min⁻¹) at a heating rate of 10 °C min⁻¹ up to 250 °C.

Fourier Transformed Infrared (FT-IR). Fourier Transformed Infrared (FT-IR) spectra were recorded on a 6700 FT-IR Nicolet spectrophotometer, using diamond ATR technique. The spectra were recorded on non-diluted compounds in the range 400-4000 cm^{-1} . ATR correction was applied.

UV-Vis spectra. UV-Vis spectra of powdered compounds have been collected by using a Perkin-Elmer Lambda 750 spectrophotometer equipped with a powder sample holder set. The UV-Vis spectra of solutions were recorded on a Perkin-Elmer Lambda-750 using calibrated 1 cm Quartz-cell.

Energy-dispersive X-ray spectroscopy. EDX measurements were performed using a SEM-FEG (Scanning Electron Microscope enhanced by a Field Emission Gun) equipment (JSM 7001-F, Jeol). The measurements were acquired with a SDD XMax 50 mm² detector and the Aztec (Oxford) system working at 15 kV and 10 mm distance. The quantification is realized with the standard library provided by the constructor using $L\alpha$ lines.

Electrochemistry. Cyclic voltammetric (CV) experiments were carried out with an EG&G 273 A driven by a PC with the M270 software. Measurements were performed at room temperature in a conventional single compartment cell. A glassy carbon (GC) electrode with a diameter of 3 mm was used as the working electrode. The auxiliary electrode was a Pt plate placed within a fritted-glass isolation chamber and potentials are quoted against a saturated calomel electrode (SCE). The solutions were deaerated thoroughly for at least 10 minutes with pure argon and kept under a positive pressure of this gas during the experiments.

b) Synthetic methods

General information. The compounds described herein, were synthesized from aqueous mixtures of gamma-cyclodextrin (CD; TCI, 99%). The starting chemical reactants were commercially available and were used without any further purification except the water-soluble salts of octahedral molybdenum clusters.

i. Preparation of water-soluble salts of $\{[\text{Mo}_6\text{X}_8\text{Cl}^a_6]@2\text{CD}\}^{2-}$

Water soluble salts of octahedral molybdenum clusters, $\text{Na}_2[\text{Mo}_6\text{X}_8\text{Cl}^a_6]\cdot\text{Me}_2\text{CO}$ with X= Br or I, have been prepared by metathesis of $(\text{TBA})_2[\text{Mo}_6\text{X}_8\text{Cl}^a_6]$ with sodium tetraphenylborate.

Synthesis of $(\text{TBA})_2[\text{Mo}_6\text{I}_8\text{Cl}^a_6]$: The cluster $(\text{TBA})_2[\text{Mo}_6\text{I}_8\text{Cl}^a_6]$ was obtained using a modified published procedure.⁴ $(\text{TBA})_2[\text{Mo}_6\text{I}_8(\text{NO}_3)^a_6]$ (1 g, 0.407 mmol) was dissolved in 100 mL of acetone and 1 mL of concentrated hydrochloric acid was added. The resulting solution was boiled for several hours. An orange precipitate occurred during the reaction, and its dissolution indicated that the reaction was complete. The resulting solution was evaporated to a minimum volume and the complex was precipitated by diethyl ether. The resulting crystalline powder (sometimes oil) was washed several times with water, dried, dissolved in 150 ml of acetone and evaporated to dryness to form red crystals of $(\text{TBA})_2[\text{Mo}_6\text{I}_8\text{Cl}^a_6]$. Yield 0.84 g (90%). Anal. Calcd for $\text{C}_{32}\text{H}_{72}\text{Cl}_6\text{I}_8\text{Mo}_6\text{N}_2$: C, 16.71; H, 3.16; N, 1.22. Found: C, 16.6; H, 3.2; N, 1.3. EDS shows Mo : I : Cl ratio = 6 : 8.1 : 6.1.

Synthesis of $(\text{TBA})_2[\text{Mo}_6\text{Br}_8\text{Cl}^a_6]$: Similar procedure than compound $(\text{TBA})_2[\text{Mo}_6\text{I}_8\text{Cl}^a_6]$, using $(\text{TBA})_2[\text{Mo}_6\text{Br}_8(\text{NO}_3)^a_6]$ (1 g, 0.482 mmol). Precipitation stage was not observed during the reaction, so the reaction was carried out for 2 hours. Yield 0.848 g (92%). Anal. Calcd for $\text{C}_{32}\text{H}_{72}\text{Cl}_6\text{Br}_8\text{Mo}_6\text{N}_2$: C, 20.07; H, 3.79; N, 1.46. Found: C, 20.1; H, 3.8; N, 1.3. EDS shows Mo : Br : Cl ratio = 6 : 7.8 : 6.1.

Synthesis of $\text{Na}_2[\text{Mo}_6\text{Br}_8\text{Cl}^a_6]\cdot\text{Me}_2\text{CO}$: $(\text{TBA})_2[\text{Mo}_6\text{Br}_8\text{Cl}^a_6]$ (0.2 g, 0.105 mmol) was dissolved in 40 mL of dichloromethane. NaBPh_4 (0.143 g, 0.418 mmol) was added under vigorous stirring to the solution of the complex. The process of precipitating the reaction product was accelerated by placing the reaction mixture in an ultrasonic bath for 10 minutes. The resulting powder was separated from the solution, washed several times with dichloromethane and dissolved in a minimum amount of acetone (~ 10 mL). The solution was filtered from insoluble compounds and added under stirring to 50 mL of diethyl ether. The resulting complex $\text{Na}_2[\text{Mo}_6\text{Br}_8\text{Cl}^a_6]\cdot\text{Me}_2\text{CO}$ was separated from the solution, washed with diethyl ether and dried in air. The resulting compound was sensitive to air water. Yield 0.144 g (90%). EDS shows Mo : Br : Cl : Na = 6 : 7.9 : 6.0 : 2.1. TGA (figure S31) revealed a weight loss of about 2.8% from 30 to 100 °C (the calculated weight loss of acetone molecule is 3.8%).

Synthesis of $\text{Na}_2[\text{Mo}_6\text{I}_8\text{Cl}^a_6]\cdot 2\text{Me}_2\text{CO}$: Similar procedure than compound $\text{Na}_2[\text{Mo}_6\text{Br}_8\text{Cl}^a_6]\cdot\text{Me}_2\text{CO}$, using $(\text{TBA})_2[\text{Mo}_6\text{I}_8\text{Cl}^a_6]$ (0.2 g, 0.087 mmol) and NaBPh_4 (0.119 g, 0.348 mmol). Yield 0.155 g (90 %). EDS shows Mo : I : Cl : Na ratio = 6 : 8.0 : 6.1 : 1.9. TGA (figure S31) revealed a weight loss of about 5.0% from 30 to 100 °C (the calculated weight loss of 2 acetone molecules is 5.9%).

ii. Preparation of the compounds built from $\{[Mo_6X_i_8Cl^a_6]@2CD\}^{2-}$

Synthesis of $Na_2\{[Mo_6Br^i_8Cl^a_6]@2CD\} \cdot 3NaCl \cdot 10H_2O$ (noted 1-Br): $Na_2[Mo_6Br^i_8Cl^a_6] \cdot Me_2CO$ (0.15 g, 0.098 mmol), CD (0.275 g, 0.196 mmol), NaCl (50 mg, 0.85 mmol) were dissolved in 3 mL of water under stirring. During the slow evaporation of the solution, crystals (yellow lozenge plates) of the compound **1-Br** were formed after a day, which were separated from the solution by filtration, then washed with a small amount of cold water and ethanol, and dried in air. Yield: 52 % based on octahedral clusters. EDS shows Mo : Br : Cl : Na ratio = 6 : 8.5 : 8.5 : 4.8. TGA (figure S31) revealed a weight loss of about 4.2% from RT to 150 °C (the calculated weight loss of 10 H₂O is 4%).

Sodium chloride was added to the reaction mixture in order to get good quality crystals. Crystals having similar unit cells are obtained also without adding NaCl, but the quality of the resulting crystals is poor.

Synthesis of $Na_2\{[Mo_6I^i_8Cl^a_6]@2CD\} \cdot 3NaCl \cdot 10H_2O$ (noted 1-I): $Na_2[Mo_6I^i_8Cl^a_6] \cdot 2Me_2CO$ (0.15 g, 0.076 mmol), CD (213 g, 0.152 mmol), NaCl (50 mg, 0.85 mmol) were dissolved in 3 mL of water under stirring. As for **1-Br**, the addition of sodium chloride provides better quality crystals. During the slow evaporation of the solution, crystals (orange/red lozenge plates) of the compound **1-I** were formed after a day, which were separated from the solution by filtration, then washed with a small amount of cold water and ethanol, and dried in air. Yield: 58 % based on octahedral clusters. EDS shows Mo : I : Cl : Na ratio = 6 : 6.8 : 8.6 : 6.6. TGA (figure S31) revealed a weight loss of about 4% from RT to 150 °C (the calculated weight loss of 10 H₂O is 3.7%).

Synthesis of $Na_2\{[Mo_6Br^i_8Cl^a_6]@2CD\} \cdot CD \cdot 45H_2O$ (noted 2-Br): $Na_2[Mo_6Br^i_8Cl^a_6] \cdot Me_2CO$ (0.15 g, 0.098 mmol) and γ -CD (0.412 g, 0.294 mmol) were dissolved in 3 mL of water under stirring. During the slow evaporation of the solution, crystals (yellow square plates) of the compound **2-Br** were formed after a day, which were separated from the solution by filtration, then washed with a small amount of cold water and ethanol, and dried in air. Yield: 61 % based on octahedral clusters. EDS shows Mo : Br : Cl : Na ratio = 6 : 8 : 6.1 : 1.9. TGA (figure S31) revealed a weight loss of about 13% from RT to 150 °C (the calculated weight loss of 45 H₂O is 13.2%).

Synthesis of $Na_2\{[Mo_6I^i_8Cl^a_6]@2CD\} \cdot CD \cdot 45H_2O$ (noted 2-I): $Na_2[Mo_6I^i_8Cl^a_6] \cdot 2Me_2CO$ (0.15 g, 0.076 mmol) and γ -CD (0.320 g, 0.228 mmol) were dissolved in 3 mL of water under stirring. During the slow evaporation of the solution, crystals (orange square plates) of the compound **2-I** were formed after a day, which were separated from the solution by filtration, then washed with a small amount of cold water and ethanol, and dried in air. Yield: 71 % based on octahedral clusters. EDS shows Mo : I : Cl : Na ratio = 6 : 7.1 : 5.8 : 2.8. TGA (figure S31) revealed a weight loss of about 11.5% from RT to 150 °C (the calculated weight loss of 45 H₂O is 12.4%).

iii. Preparation of the compounds built from $\{Mo_6X_i_8Cl^a_6@2CD\}^{2-}$ and $\{Al_{13}\}^{7+}$

Preparation of the stock solution of $\{Al_{13}\}^{7+}$: The solution of $\{Al_{13}\}^{7+}$ polycations was obtained using a modified published procedure⁵. 100 ml of 0.25 M aluminum chloride solution was heated and was kept at 70 °C using a thermostat. Within 15 minutes, 240 ml of 0.25 M NaOH solution was added drop by drop under continuous stirring. Then the solution was cooled down to 20 °C. The $\{Al_{13}\}^{7+}$ concentration of the resulting solution is about 5.5 mM.

Synthesis of $\{\text{Al}_{13}\}\{\text{Mo}_6\text{Br}_8\text{Cl}_6^{\text{a}}\}@2\text{CD}\}\text{Cl}_5\cdot 60\text{H}_2\text{O}$ (noted **3-Br)** : $\text{Na}_2\{[\text{Mo}_6\text{Br}_8\text{Cl}_6^{\text{a}}]\}@2\text{CD}\}\cdot 3\text{NaCl}\cdot 10\text{H}_2\text{O}$ (0.1 g, 0.022 mmol) were dissolved in 4 mL of stock solution of $\{\text{Al}_{13}\}^{7+}$ polycations (0.022 mmol) under vigorous stirring in order to obtain orange clear solution. During the slow evaporation of the solution, large crystals (orange hexagonal bipyramids) of the compound **3-Br** were formed after 2 days, which were separated from the solution by filtration, then washed with a small amount of cold water and ethanol, and dried in air. Yield: 47 % based on octahedral clusters. EDS shows Al : Mo : Br : Cl ratio = 13 : 7.2 : 8.3 : 10.6. TGA (figure S31) revealed a weight loss of about 19 % from RT to 150 °C (the calculated weight loss of 60 H₂O is 20%)

Synthesis of $\{\text{Al}_{13}\}\{\text{Mo}_6\text{I}_8\text{Cl}_6^{\text{a}}\}@2\text{CD}\}\text{Cl}_5\cdot 60\text{H}_2\text{O}$ (noted **3-I)** : $\text{Na}_2\{[\text{Mo}_6\text{I}_8\text{Cl}_6^{\text{a}}]\}@2\text{CD}\}\cdot 3\text{NaCl}\cdot 10\text{H}_2\text{O}$ (0.1 g, 0.02 mmol) were dissolved in 4 mL of stock solution of $\{\text{Al}_{13}\}^{7+}$ polycations (0.022 mmol) under vigorous stirring in order to obtain orange clear solution. During the slow evaporation of the solution, large crystals (red hexagonal bipyramids) of the compound **3-I** were formed after 2 days, which were separated from the solution by filtration, then washed with a small amount of cold water and ethanol, and dried in air. Yield: 53 % based on octahedral clusters. EDS shows Al : Mo : I : Cl ratio = 13 : 6.8 : 7.1 : 11.1. TGA (figure S31) revealed a weight loss of about 18 % from RT to 150 °C (the calculated weight loss of 60 H₂O is 19%).

2. Single-crystal X-ray diffraction

a) Crystallographic parameters for 1-Br and 1-I

Table S1: Crystal data and structure refinement for **1-Br** and **1-I**

Identification code	1-Br	1-I
Empirical formula	$C_{96}H_{112}Br_8Cl_8Mo_6Na_5O_{102.5}$	$C_{96}H_{112}Cl_8Mo_6Na_{4.5}O_{107}$
Formula weight	4519.32	4955.74
Temperature/K	150.15	200(2)
Crystal system	Monoclinic	Monoclinic
Space group	$P2_1$	$P2_1$
a/Å	15.8501(17)	15.8187(9)
b/Å	32.821(4)	32.856(2)
c/Å	17.405(2)	17.4013(11)
$\alpha/^\circ$	90	90
$\beta/^\circ$	93.734(4)	93.728(2)
$\gamma/^\circ$	90	90
Volume/Å ³	9035.4(18)	9025.0(9)
Z	2	2
ρ_{calc}/cm^3	1.661	1.824
μ/mm^{-1}	2.402	2.004
F(000)	4462	4811
Crystal size/mm ³	0.32 × 0.24 × 0.03	0.2 × 0.16 × 0.03
Radiation	MoK α ($\lambda = 0.71073$)	MoK α ($\lambda = 0.71073$)
2 θ range for data collection/ $^\circ$	4.184 to 55.05	3.598 to 54.284
Index ranges	-18 ≤ h ≤ 20, -42 ≤ k ≤ 42, -22 ≤ l ≤ 22	-20 ≤ h ≤ 14, -42 ≤ k ≤ 42, -22 ≤ l ≤ 22
Reflections collected	113359	238942
Independent reflections	40804 [$R_{int} = 0.0347$, $R_{sigma} = 0.0565$]	39940 [$R_{int} = 0.0717$, $R_{sigma} = 0.0620$]
Data/restraints/parameters	40804/37/2109	39940/19/1984
Goodness-of-fit on F ²	1.034	1.034
Final R indexes [$I \geq 2\sigma(I)$]	$R_1 = 0.0593$, $wR_2 = 0.1701$	$R_1 = 0.0484$, $wR_2 = 0.1230$
Final R indexes [all data]	$R_1 = 0.0713$, $wR_2 = 0.1817$	$R_1 = 0.0755$, $wR_2 = 0.1423$
Largest diff. peak/hole / e Å ⁻³	2.59/-1.38	2.44/-1.17
Flack parameter	0.028(8)	-0.013(5)

b) Crystallographic parameters for 2-Br and 2-I

Table S2: Crystal data and structure refinement for 2-Br and 2-I

Identification code	2-Br	2-I
Empirical formula	$C_{144}H_{168}Br_8Cl_6Mo_6Na_4O_{138}$	$C_{144}H_{168}Cl_6I_8Mo_6O_{138}$
Formula weight	5626.35	5910.31
Temperature/K	200(2)	200(2)
Crystal system	Tetragonal	Tetragonal
Space group	<i>I</i> 422	<i>I</i> 422
<i>a</i> /Å	23.715(2)	23.7708(16)
<i>b</i> /Å	23.715(2)	23.7708(16)
<i>c</i> /Å	56.802(5)	57.456(4)
α /°	90	90
β /°	90	90
γ /°	90	90
Volume/Å ³	31945(7)	32465(5)
<i>Z</i>	4	4
ρ_{calc} /cm ³	1.17	1.209
μ /mm ⁻¹	1.362	1.111
<i>F</i> (000)	11256	11656
Crystal size/mm ³	0.09 × 0.07 × 0.03	0.25 × 0.22 × 0.15
Radiation	MoK α (λ = 0.71073)	MoK α (λ = 0.71073)
2 θ range for data collection/°	1.86 to 54.134	1.418 to 53.016
Index ranges	-30 ≤ <i>h</i> ≤ 20, -15 ≤ <i>k</i> ≤ 30, -65 ≤ <i>l</i> ≤ 72	-29 ≤ <i>h</i> ≤ 29, -29 ≤ <i>k</i> ≤ 29, -71 ≤ <i>l</i> ≤ 72
Reflections collected	68002	477901
Independent reflections	17521 [<i>R</i> _{int} = 0.1861, <i>R</i> _{sigma} = 0.2521]	16718 [<i>R</i> _{int} = 0.1173, <i>R</i> _{sigma} = 0.0384]
Data/restraints/parameters	17521/54/302	16718/25/314
Goodness-of-fit on <i>F</i> ²	0.988	1.065
Final <i>R</i> indexes [<i>I</i> ≥ 2 σ (<i>I</i>)]	<i>R</i> ₁ = 0.1011, <i>wR</i> ₂ = 0.2643	<i>R</i> ₁ = 0.1108, <i>wR</i> ₂ = 0.2881
Final <i>R</i> indexes [all data]	<i>R</i> ₁ = 0.2301, <i>wR</i> ₂ = 0.3499	<i>R</i> ₁ = 0.1493, <i>wR</i> ₂ = 0.3443
Largest diff. peak/hole / e Å ⁻³	2.61/-2.30	1.81/-1.76
Flack parameter	0.18(3)	0.26(5)

c) Crystallographic parameters for 3-Br and 3-I

Table S3: Crystal data and structure refinement for **3-Br** and **3-I**

Identification code	3-Br	3-I
Empirical formula	C ₉₆ H ₁₁₂ Al ₁₃ Br ₈ Cl ₁₀ Mo ₆ O ₁₂₀	C ₉₆ H ₁₀₈ Al ₁₃ Cl _{8.5} I ₈ Mo ₆ O ₁₂₀
Formula weight	5106.01	5424.72
Temperature/K	200(2)	200(2)
Crystal system	Hexagonal	Hexagonal
Space group	P6 ₂ 22	P6 ₂ 22
a/Å	19.805(2)	19.751(2)
b/Å	19.805(2)	19.751(2)
c/Å	57.843(7)	57.616(7)
α/°	90	90
β/°	90	90
γ/°	120	120
Volume/Å ³	19649(5)	19465(5)
Z	3	3
ρ _{calc} /cm ³	1.295	1.388
μ/mm ⁻¹	1.723	1.443
F(000)	7557	7900
Crystal size/mm ³	0.2 × 0.2 × 0.15	0.25 × 0.22 × 0.13
Radiation	MoKα (λ = 0.71073)	MoKα (λ = 0.71073)
2θ range for data collection/°	5.898 to 54.97	4.124 to 55.774
Index ranges	-25 ≤ h ≤ 25, -25 ≤ k ≤ 24, -75 ≤ l ≤ 66	-25 ≤ h ≤ 25, -24 ≤ k ≤ 25, -65 ≤ l ≤ 75
Reflections collected	190540	189091
Independent reflections	15048 [R _{int} = 0.1000, R _{sigma} = 0.0613]	15487 [R _{int} = 0.0799, R _{sigma} = 0.0421]
Data/restraints/parameters	15048/29/321	15487/12/291
Goodness-of-fit on F ²	1.022	1.738
Final R indexes [I >= 2σ (I)]	R ₁ = 0.0920, wR ₂ = 0.2458	R ₁ = 0.1367, wR ₂ = 0.3625
Final R indexes [all data]	R ₁ = 0.1333, wR ₂ = 0.2923	R ₁ = 0.1638, wR ₂ = 0.4039
Largest diff. peak/hole / e Å ⁻³	1.82/-0.93	3.04/-4.74
Flack parameter	0.26(2)	0.28(5)

d) Crystallographic parameters of molecular clusters observed in the compounds 1-Br, 1-I, 2-Br, 2-I, 3-Br and 3-I

Table S4: Bond distances of $[\text{Mo}_6\text{Br}_8\text{Cl}^a_6]^{2-}$ cluster observed in the compounds **1-Br**, **2-Br** and **3-Br**

Compound	1-Br	2-Br	3-Br
Mo-Mo (Å)	2.623(1) - 2.6388(2)	2.631(3) - 2.638(2)	2.628(2) - 2.632(2)
Mo-Br (Å)	2.591(2) - 2.614(2)	2.603(3) - 2.633(3)	2.5949(18) - 2.621(2)
Mo-Cl (Å)	2.424(3) - 2.438(3)	2.432(5) - 2.503(12)	2.421(4) - 2.519(8)

Table S5: Bond distances of $[\text{Mo}_6\text{I}_8\text{Cl}^a_6]^{2-}$ cluster observed in the compounds **1-I**, **2-I** and **3-I**

Compound	1-I	2-I	3-I
Mo-Mo (Å)	2.654(2) - 2.678(2)	2.6525(4) - 2.693(3)	2.670(3) - 2.693(3)
Mo-I (Å)	2.772(2) - 2.793(2)	2.771(3) - 2.807(3)	2.773(2) - 2.796(2)
Mo-Cl (Å)	2.426(5) - 2.464(4)	2.312(2) - 2.410(2)	2.398(6) - 2.460(6)

Table S6 : Al-O bond distances in **3-Br** and **3-I**. A representation of the aluminum polycation is represented in figure S1.

Compound	3-Br	3-I
Al^{central}-O (Å)	1.85(2)	1.87(2)
Al peripheral-O (Å)	1.98(2) - 2.01(2)	1.97(2) - 2.06(2)
Al-OH (Å)	1.77(2) - 1.90(2)	1.71(1) - 2.00 (1)
Al-H₂O (Å)	1.96 (1) - 2.01 (1)	1.88(2) - 1.89(2)

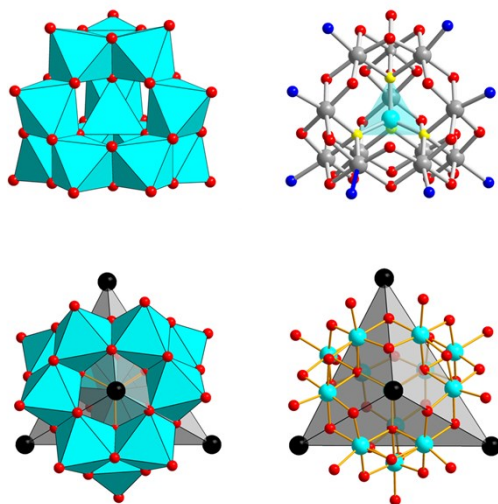


Figure S1: (Top) Illustration of the $\{Al_{13}\}^{7+}$ building block which adopts a ϵ -Keggin arrangement. The μ_4 -oxo, μ_2 -hydroxo and terminal water molecules are in yellow, red and blue, respectively. (Bottom) Illustration of the super-tetrahedron defined by one $\{Al_{13}\}^{7+}$ and the four chlorine atoms capping it. Each chlorine atom is linked to three hydroxo groups with an average distance about 3.25 Å. The edge size of this $\{Al_{13}\}Cl_4$ super-tetrahedra are in the range 8.6-9.1 Å, which adopts a ϵ -Keggin arrangement

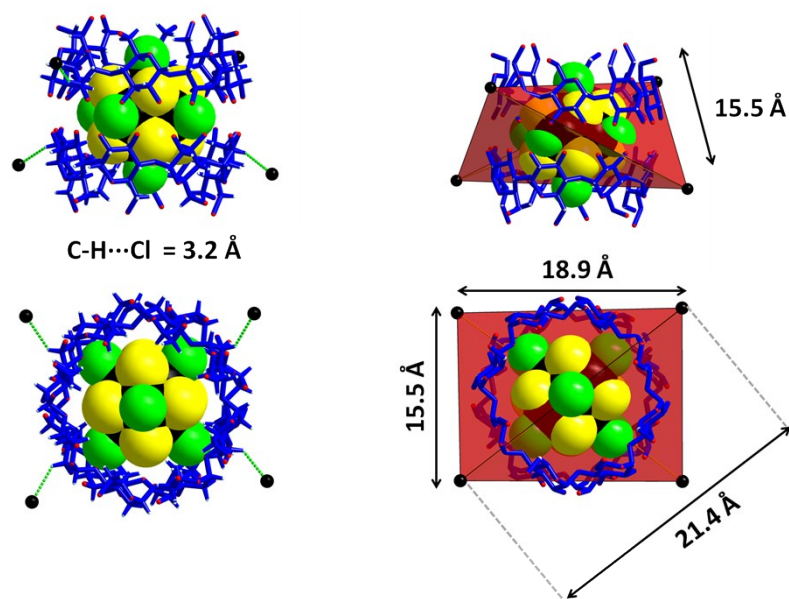


Figure S2: Illustration of the $\{Mo_6\}Cl_4$ super-tetrahedron. This illustration corresponds to $\{Mo_6\}Cl_4$ super-tetrahedron observed in **3-Br**, the polyhedron is same in **3-I** except the orientation of the Mo6 based cluster.

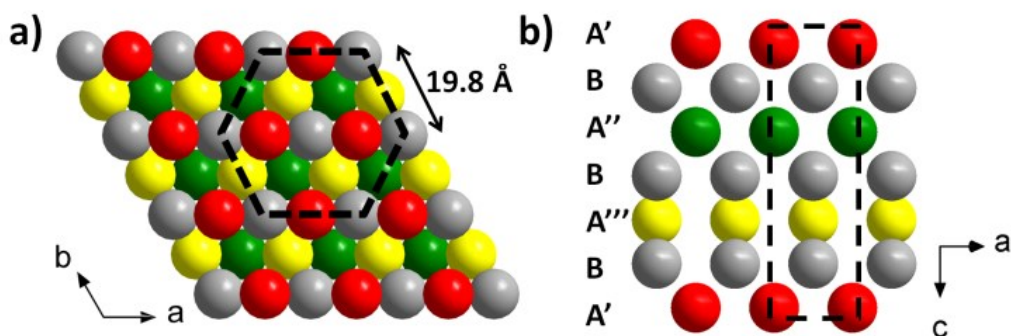


Figure S3: a and b) Schematic views of the crystal packing of **3** along in the *bc* plane (a) and *ac* plane (b) showing the unusual packing of hexagonal layers of clusters. Color code: $\{Al_{13}\}^{7+}$ are in grey, molybdenum clusters are in yellow, green or red.

a) Views of the disordered clusters $[Mo_6I_6Cl_6]^{2-}$ in **2-I** and **3-I**

The cluster $[Mo_6I_6Cl_6]^{2-}$ is disordered on different position in the crystal structures **2-I** and **3-I**. The figure S2 shows the two positions of $[Mo_6I_6Cl_6]^{2-}$ in the structure **2-I**. Both have been refined with an occupancy of 50% for each cluster. Importantly the supramolecular adducts $\{[Mo_6I_6Cl_6]@2CD\}^{2-}$ adopt the α -isomer. The crystal structure analysis of **3-I** reveals a more complex situation since the cluster is disordered over 5 positions. One of them exhibits high occupancy (75%) rather than the others have low occupancy (6.25%). In each case, the α -isomer is observed.

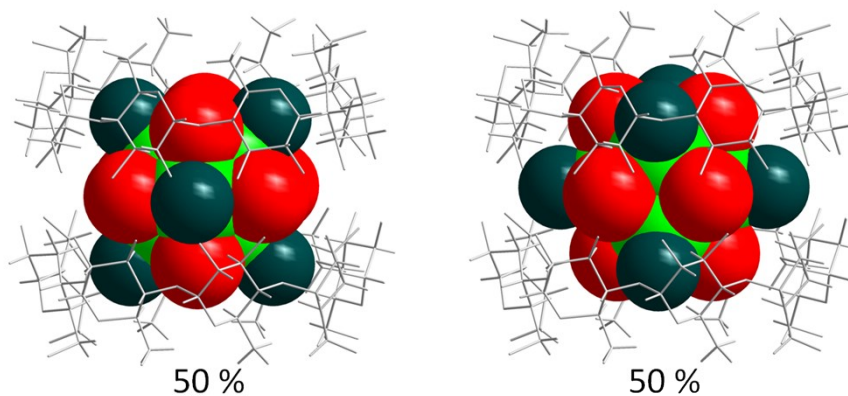


Figure S4. View of the disordered clusters $[Mo_6I_6Cl_6]^{2-}$ in **2-I**.

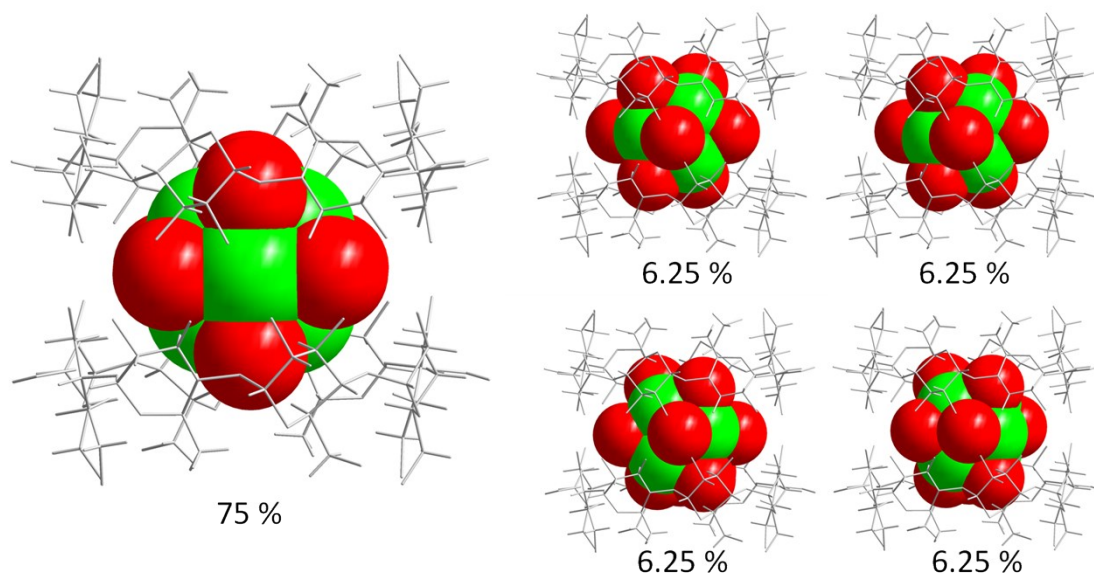


Figure S5. View of the disordered clusters $[\text{Mo}_6\text{I}_8\text{Cl}_6]^{2-}$ in **3-I**. The apical ligands (Cl) have been removed for clarity.

b) Views of the packing in the compounds **1-X** and **2-X**

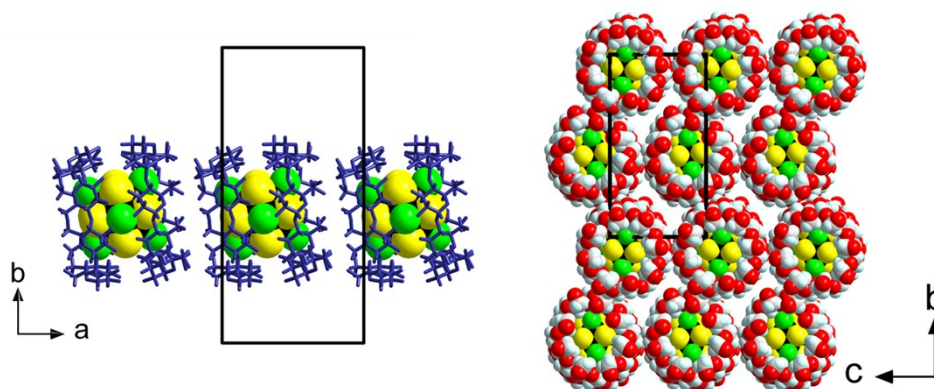


Figure S6. View of the packing of the supramolecular adduct in **1-Br** and **1-I**.

The supramolecular adducts $\{[\text{Mo}_6\text{X}_6\text{Cl}_6]@2\text{CD}\}^{2-}$ ($\text{X} = \text{Br}$ and I) are stacked together in order to form bamboo-like arrangement along the a axis. Within this bamboo cyclodextrins adopt “head to head” fashion through hydrogen bonds involving hydroxo groups of involved entities. The bamboos are perfectly aligned along the c axis, while they formed a zig-zag arrangement along the b axis the 1D-chain. Numerous close contacts between the external walls of the CD of distinct bamboo-like arrangement insured the 3D supramolecular cohesion in the ac plane. This structural organization generates only moderate voids ($\sim 15\%$).

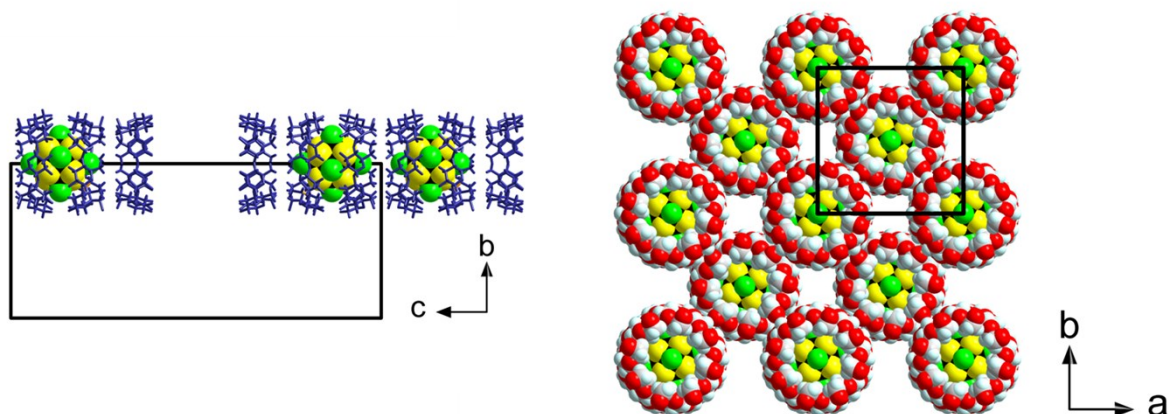


Figure S7. View of the packing of the supramolecular adduct in **2-Br**. The CDs are organized with the same fashion in the crystal structure of **2-I**; the only difference between **2-Br** and **2-I** is located on the cluster orientation (α or β -isomers).

The supramolecular adducts are stacked together in order to form fragments of bamboo-like arrangement along the c axis which built from two host-guest complexes and two free CD. This organization has been previously reported with dodecaborates⁶ and Re_6 clusters⁷ instead of Mo_6 clusters. Within this bamboo fragment, CDs are stacked together through “head to head” fashion involving hydrogen bonds between hydroxo groups of distinct macrocycle. These pseudo 1D chains form a checkerboard-like arrangement in ab plane forming one tunnel type with diameter about 5Å. Due to the presence of tunnel and “lacunary” bamboos, this structural organization generates large voids (~45%) which are filled by disordered counterions and water molecules.

c) Illustration of voids in the crystal structures

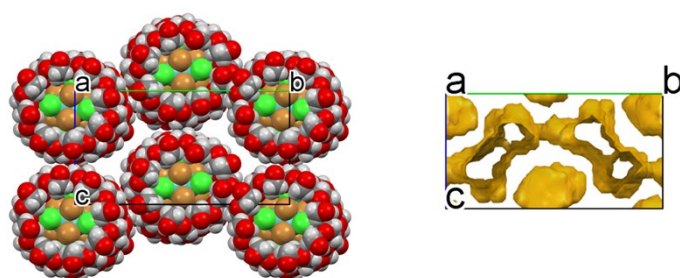


Figure S8. Illustrations of the void surfaces for the crystal structure of **1-Br** along the [100] direction. Similar voids surfaces are observed in **1-I**.

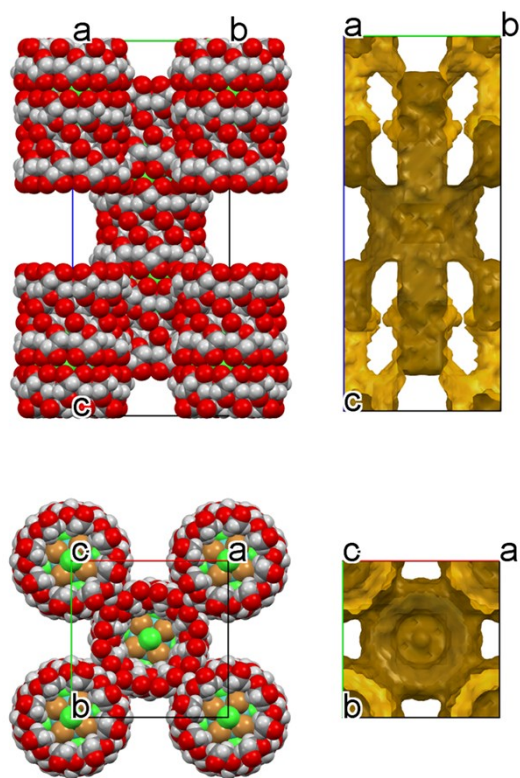


Figure S9. Illustrations of the void surfaces for the crystal structure of **2-Br** along the [100] and [001] (bottom) directions. Similar voids surfaces are observed in **2-I**.

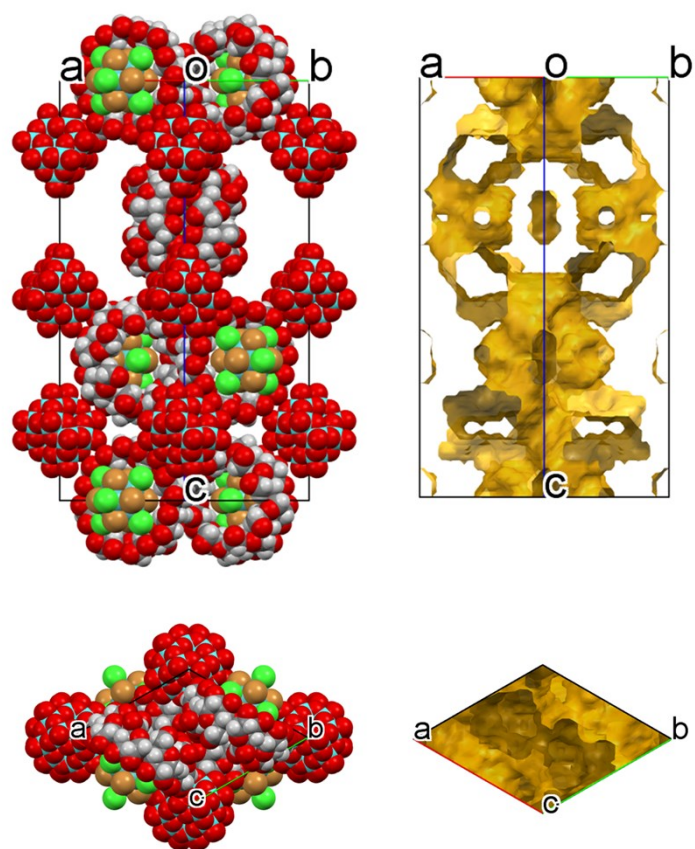


Figure S10. Illustrations of the void surfaces for the crystal structure of **3-Br** along the $[-1-10]$ (top) and $[001]$ (bottom) directions. Similar voids surfaces are observed in **3-I**.

3. ^1H NMR investigation

a) ^1H NMR titration of CD by $[\text{Mo}_6\text{Br}_8\text{Cl}_6]^{2-}$

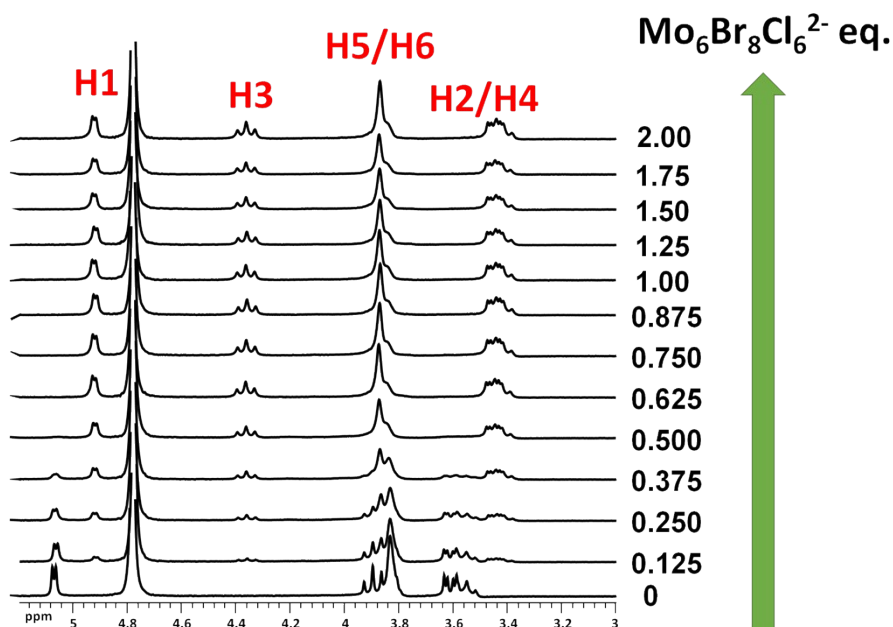


Figure S11: ^1H NMR spectra of CD in D_2O in presence of different amount of $[\text{Mo}_6\text{Br}_8\text{Cl}_6]^{2-}$. Concentration of CD = 2mM. This shows the shifting of H3 when CD is in contact with the bromine based cluster. H5 and H6 are almost not affected. We assume that this strong effect is due to the presence of the β -isomer arrangement (Fig S12) since this configuration involves short contacts between the inorganic host and the guest.

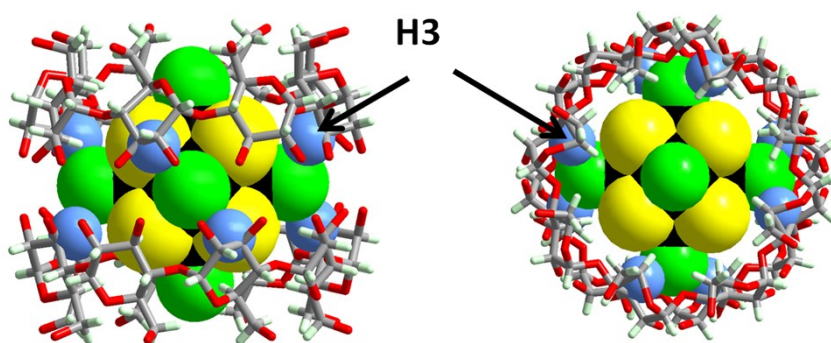


Figure S12: Illustration of the β -isomer arrangement showing the short contact between the cluster unit and the proton H3.

b) ^1H NMR titration of CD by $[\text{Mo}_6\text{I}_8\text{Cl}_6]^{2-}$

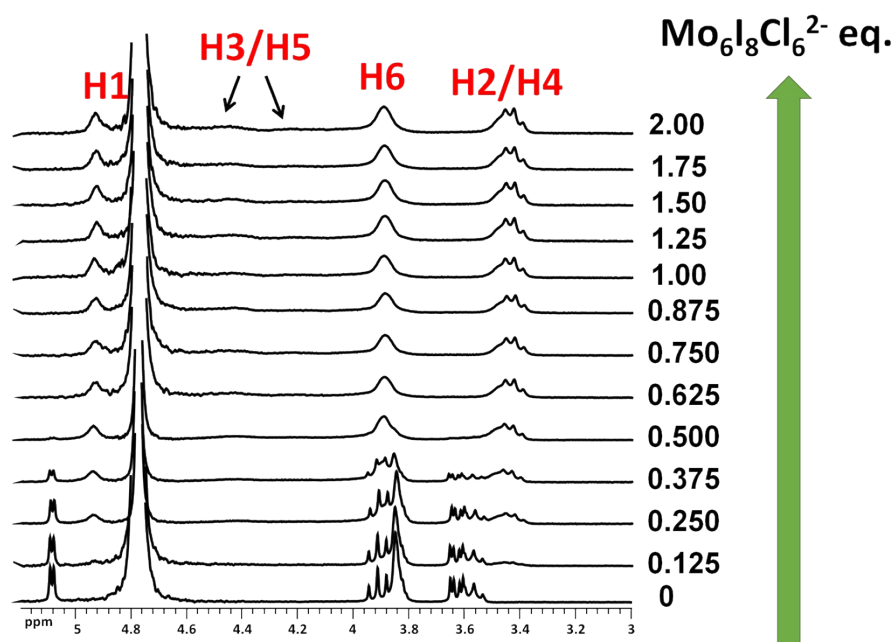


Figure S13: ^1H NMR spectra of γ -CD in D_2O in presence of different amount of $[\text{Mo}_6\text{I}_8\text{Cl}_6]^{2-}$. Concentration of CD is fixed at 2mM. This figure shows the shifting and the server linebroadening of H3 and H5 when CD is in contact with the iodine based cluster. The proton H1, H2 and H4, which are located at the exterior of the CD are slightly affected. Almost no shift is observed for H6. We assume that these strong effects are due to the presence of the α -isomer arrangement (Fig S14) since this configuration involves short contacts between the inorganic host and the guest via H3 and H5 protons.

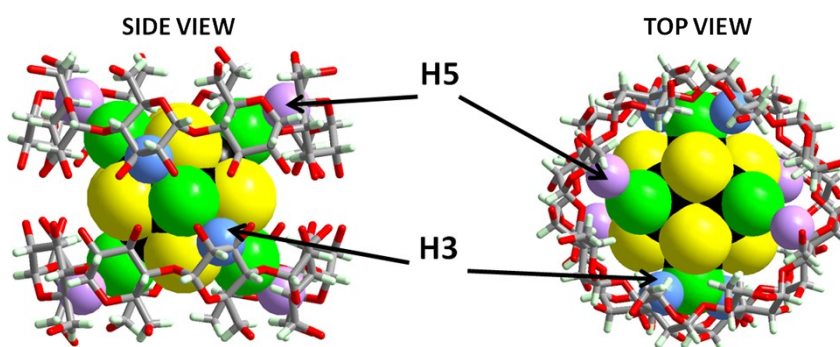


Figure S14: Illustration of the α -isomer arrangement showing the short contact between the cluster unit and the protons H3 and H5.

c) ^1H NMR titration of CD by $\{\text{Al}_{13}\}^{7+}$

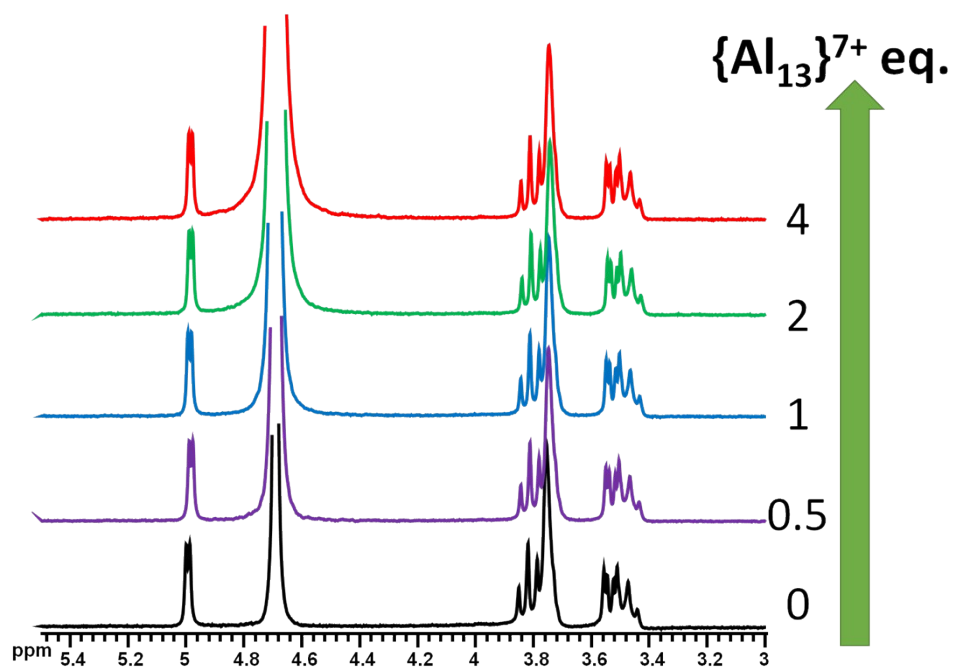


Figure S15: ^1H NMR spectra of γ -CD in D_2O in presence of different amount of $\{\text{Al}_{13}\}^{7+}$. Concentration of CD = 2mM. This figure shows that the chemical shifts of cyclodextrin are not affected by the presence of aluminium polycation, suggesting this latter does not interact with CD in aqueous solution.

4. Electrospray ionization mass spectroscopy (ESI-Mass)

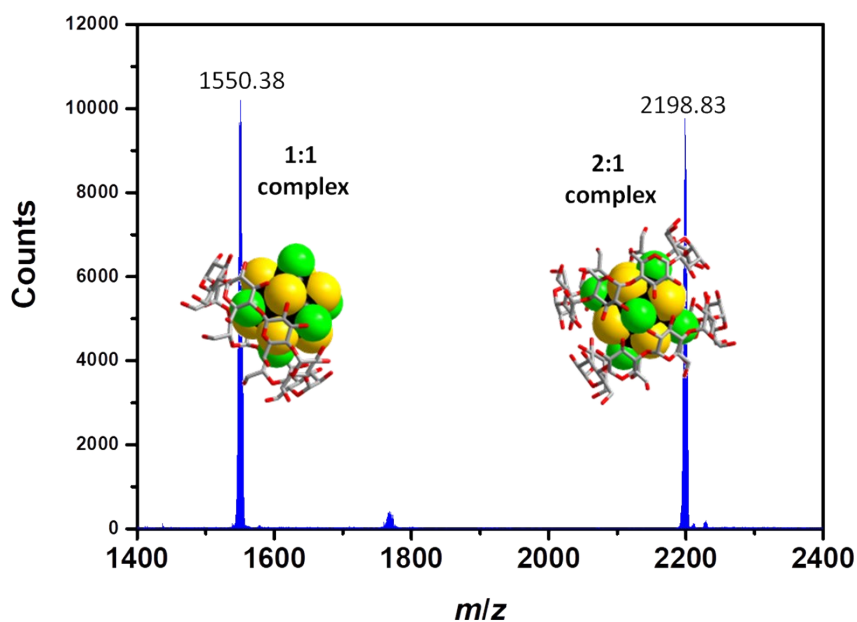


Figure S16. Fragment of the ESI-MS spectrum of the $[\text{Mo}_6\text{I}_8\text{Cl}_6]^{2-}$ in aqueous solution ($[\text{cluster}] = 20 \mu\text{M}$) containing two equivalents of CD. This shows the 1:1 ($m/z_{\text{theo}} = 1550.36$) and the 1:2 ($m/z_{\text{theo}} = 2198.92$) adducts exist in low concentration, suggesting the very high stability constant of the inclusion complex built from the encapsulation of $[\text{Mo}_6\text{I}_8\text{Cl}_6]^{2-}$ and CD.

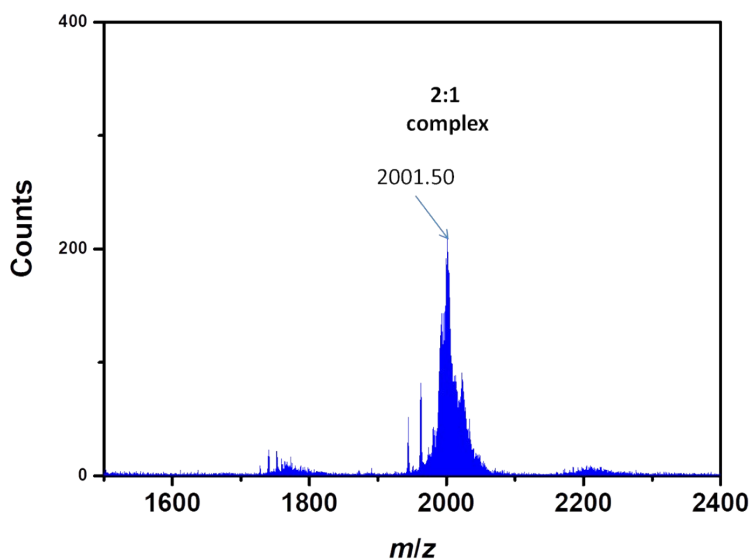


Figure S17. Fragment of the ESI-MS spectrum of the $[\text{Mo}_6\text{Br}_8\text{Cl}_6]^{2-}$ in aqueous solution ($[\text{cluster}] = 20 \mu\text{M}$) containing two equivalents of CD. This shows the large massif with a maximum corresponding to partially hydrolyzed clusters, $[\text{Mo}_6\text{Br}_8\text{Cl}_5(\text{OH})^a]^{2-}$, interacting with two CD hosts ($m/z_{\text{theo}} = 2001.69$).

5. Cyclic voltammetry experiments of the $[\text{Mo}_6\text{I}_8\text{Cl}_6]^{2-}/\text{CD}$ system in aqueous solution

a) Dependence of the peak currents upon potential scan rate

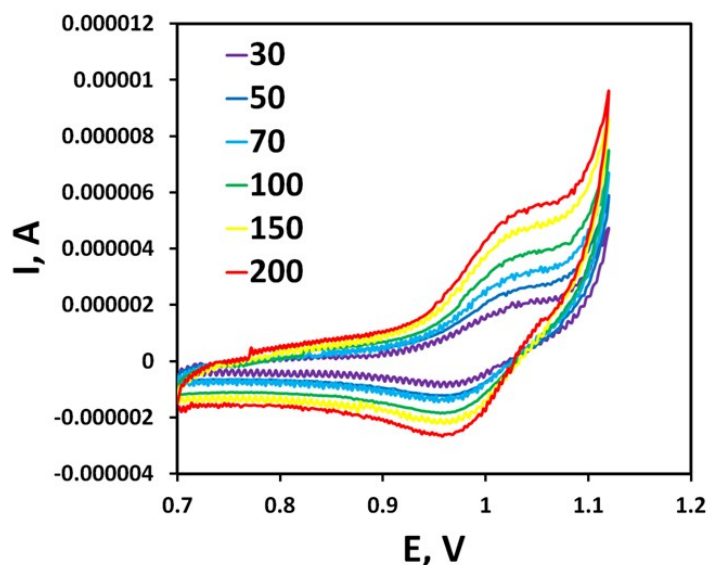


Figure S18. Cyclic voltammograms of clusters compounds $[\text{Mo}_6\text{I}_8\text{Cl}_6]^{2-}$ (10^{-3} mol.L⁻¹) in 0.025 mol.L⁻¹ HClO₄ containing two equivalent of CD per cluster ($[\text{CD}] = 2.10^{-3}$ mol.L⁻¹) at various scan rate (SR = 30-200 mV.s⁻¹). WE = glassy carbon, ref. electrode = ECS, counter electrode = Pt

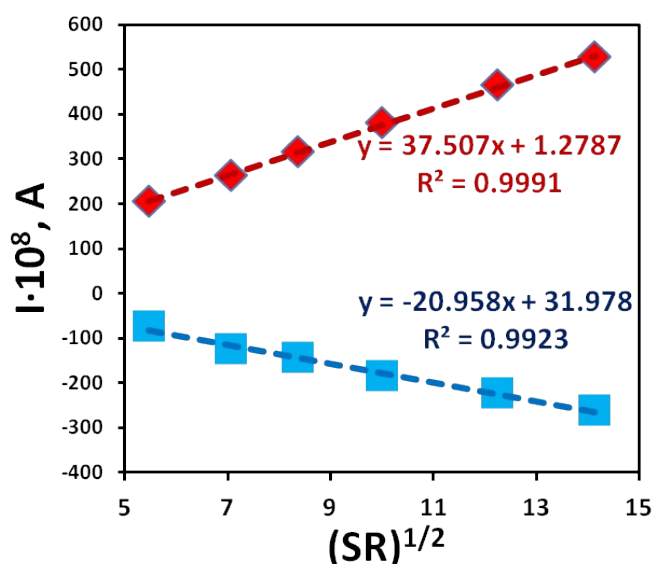


Figure S19. Linear dependence of the anodic peak current upon square root of the potential scan rate $\sqrt{\text{SR}}$.

The anodic (E_a) and cathodic (E_c) peak currents exhibits a fair linear dependence upon $\sqrt{\text{SR}}$, meaning that electron-transfer kinetic is controlled by the diffusion of redox active species at the interface.

b) Cyclic voltammetry of $[\text{Mo}_6\text{I}_8\text{Cl}^{\text{a}}]_6^{2-}$ at different concentration of CD

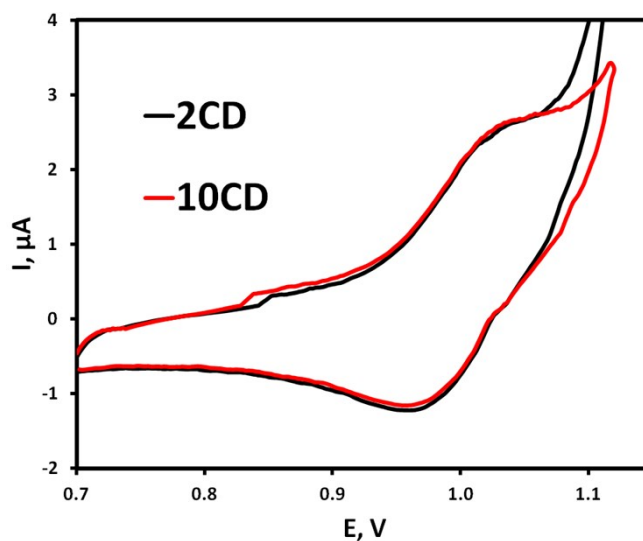


Figure S20. Cyclic voltammetry of $[\text{Mo}_6\text{I}_8\text{Cl}^{\text{a}}]_6^{2-}$ cluster in presence of 2 and 10 equivalents of gamma-cyclodextrins. Electrolyte = $0.025 \text{ mol.L}^{-1} \text{ HClO}_4$; scan rate = 50 mV.s^{-1} ; WE = glassy carbon, ref. electrode = ECS, counter electrode = Pt.

Cyclic voltammetry studies have been realized in similar cluster concentration than NMR investigations which demonstrated the presence of the supramolecular adduct $\{[\text{Mo}_6\text{I}_8\text{Cl}^{\text{a}}]_6 @ 2\text{CD}\}^{2-}$. Importantly, the one-electron redox wave is not affected by the CD concentration of CD (no shift, no decrease of intensity). This indicates that the equation of the redox coupling does not involve CD. Therefore we can conclude that the redox-coupling associate to this one-electron redox wave is $\{[\text{Mo}_6\text{I}_8\text{Cl}^{\text{a}}]_6 @ 2\text{CD}\}^{2-} / \{[\text{Mo}_6\text{I}_8\text{Cl}^{\text{a}}]_6 @ 2\text{CD}\}^-$.

6. Photo-physical investigations

a) Solid state Excitation Map of compounds 1-I, 2-I and 3-I

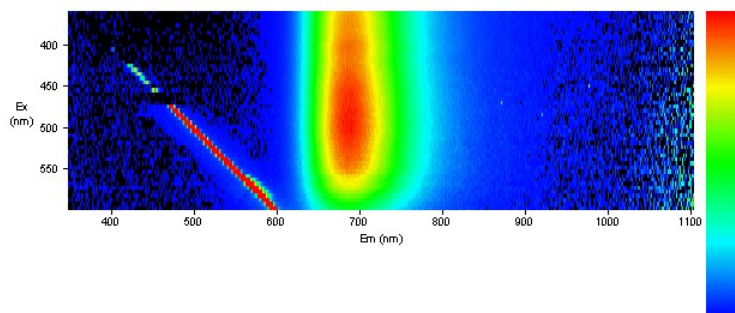


Figure S21: Solid state Excitation Map ($\Delta\lambda = 5$ nm) of **1-I**

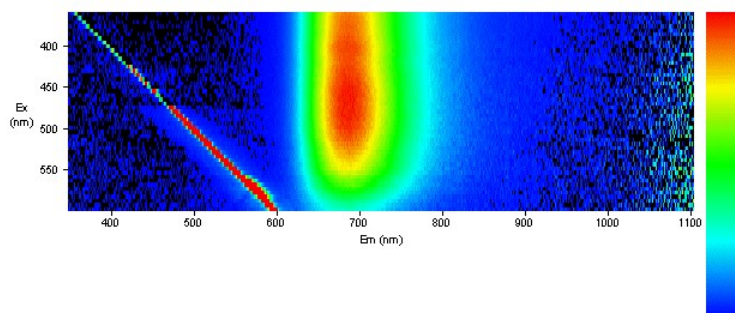


Figure S22: Solid state Excitation Map ($\Delta\lambda = 5$ nm) of **2-I**

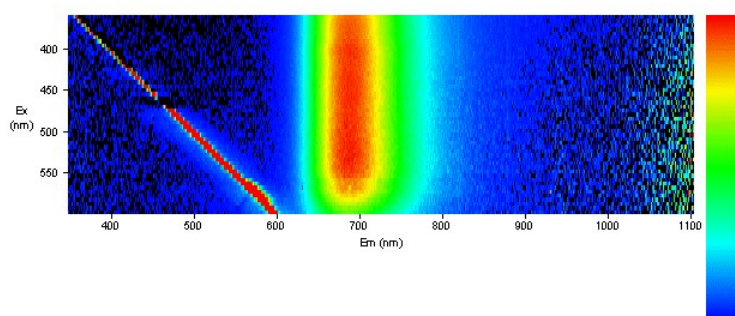


Figure S23: Solid state Excitation Map ($\Delta\lambda = 5$ nm) of **3-I**

b) Comparison of normalized emission spectra recorded in the solid-state

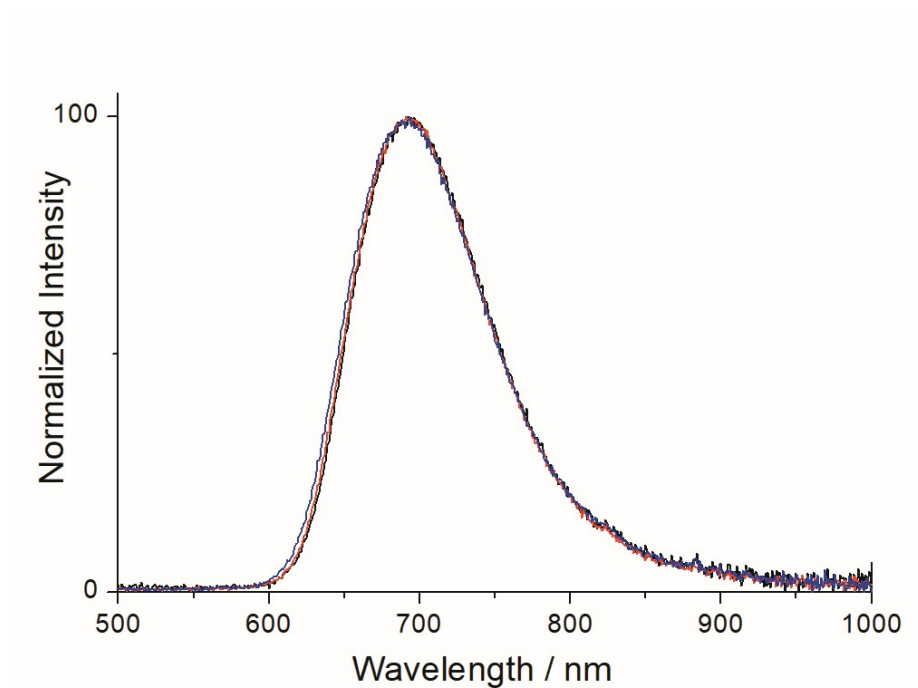


Figure S24: Normalized emission spectra recorded in the solid state ($\lambda_{\text{exc}} = 365 \text{ nm}$) for **3-I** (black), **1-I** (red) and **2-I** (blue).

c) Time resolved photoluminescence mapping of compounds 1-I, 2-I and 3-I

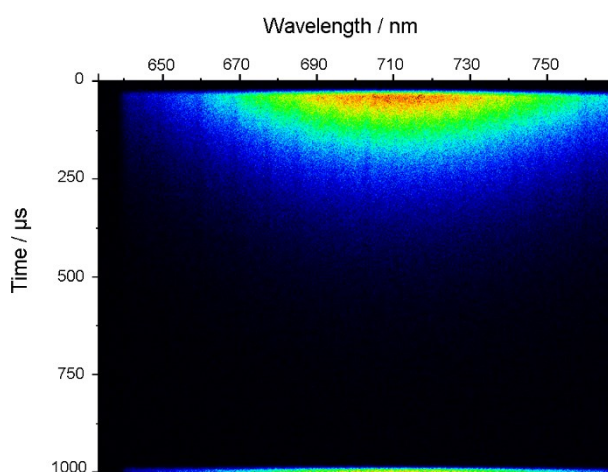


Figure S25: Time resolved photoluminescence mapping on powdered **1-I**

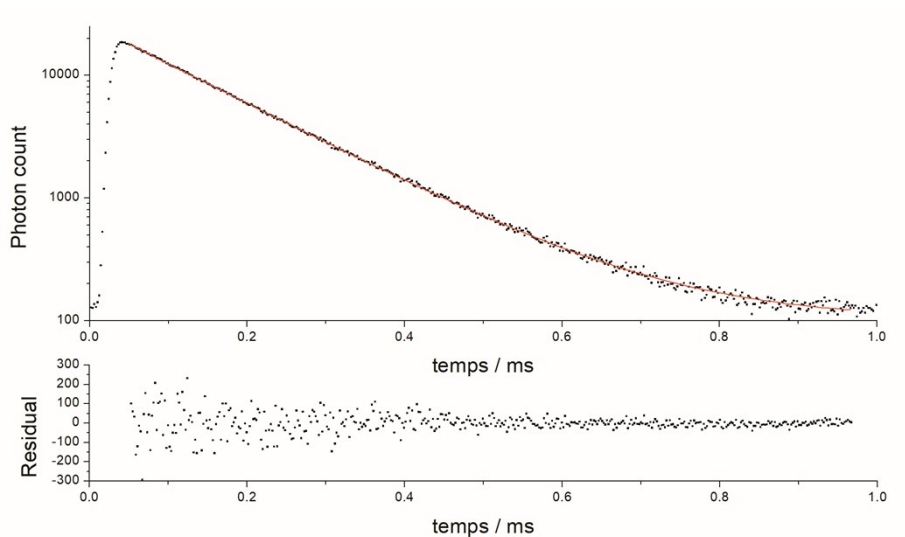


Figure S26: Fitting of the emission decay of **1-I** (mono-exponential function). $\tau_1 = 133 \mu\text{s}$; $\chi^2 = 0.99984$

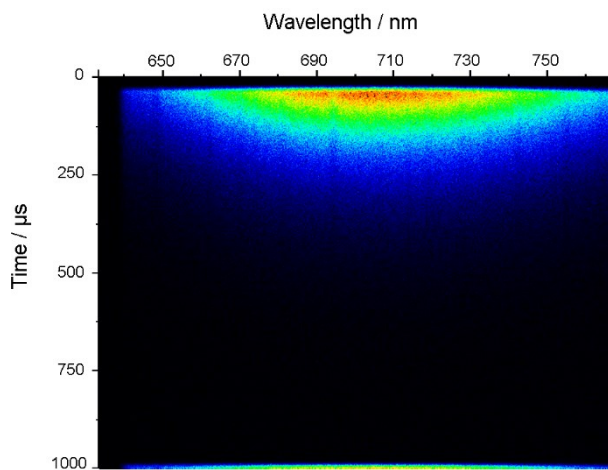


Figure S27: Time resolved photoluminescence mapping on powdered **2-I**

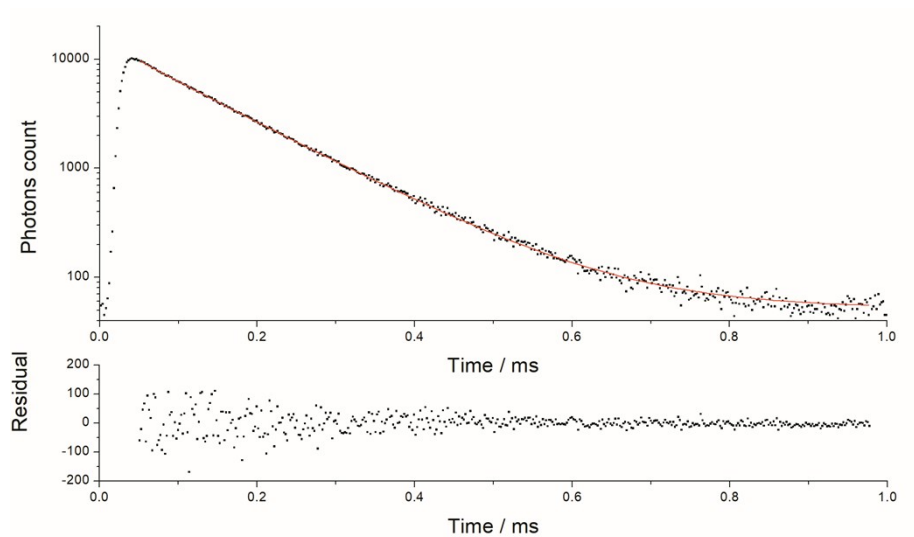


Figure S28: Fitting of the emission decay of **2-I** (bi-exponential function). $\tau_1 = 117\mu\text{s}$ (86%) and $\tau_2 = 27\mu\text{s}$ (14%) ; $\chi^2 = 0.99977$

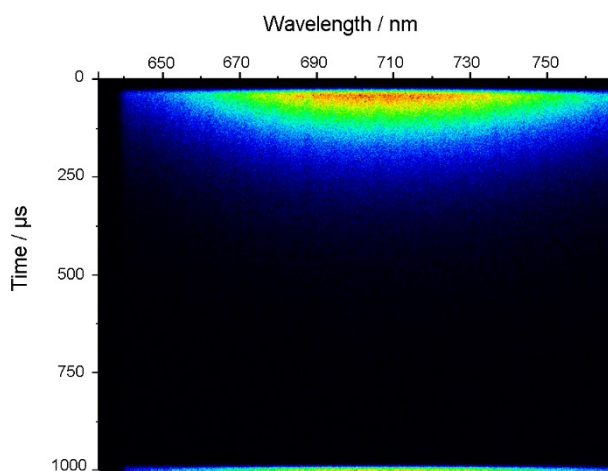


Figure S29: Time resolved photoluminescence mapping on powdered **3-I**

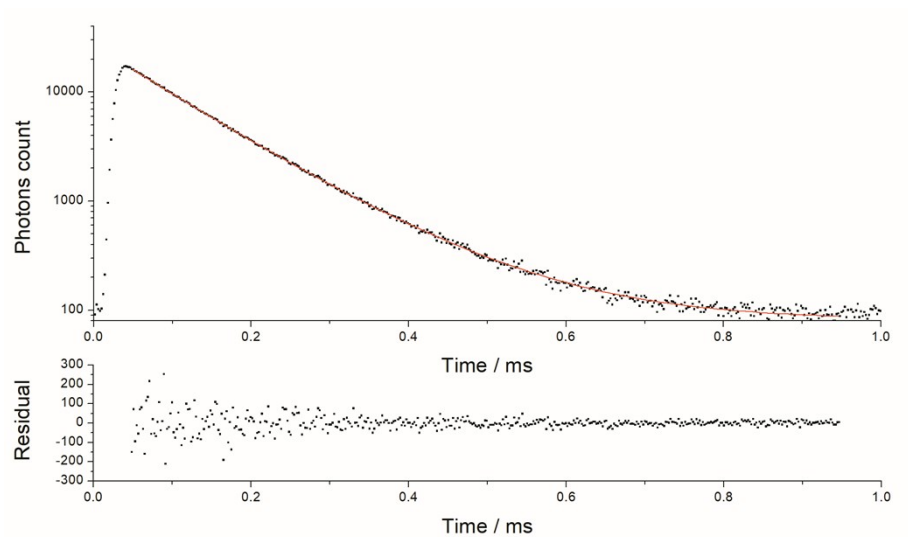


Figure S30: Fitting of the emission decay of **3-I** (bi-exponential function). $\tau_1 = 126\mu\text{s}$ (36%) and $\tau_2 = 81\mu\text{s}$ (64%) ; $\chi^2 = 0.99984$

7. Thermogravimetric analysis

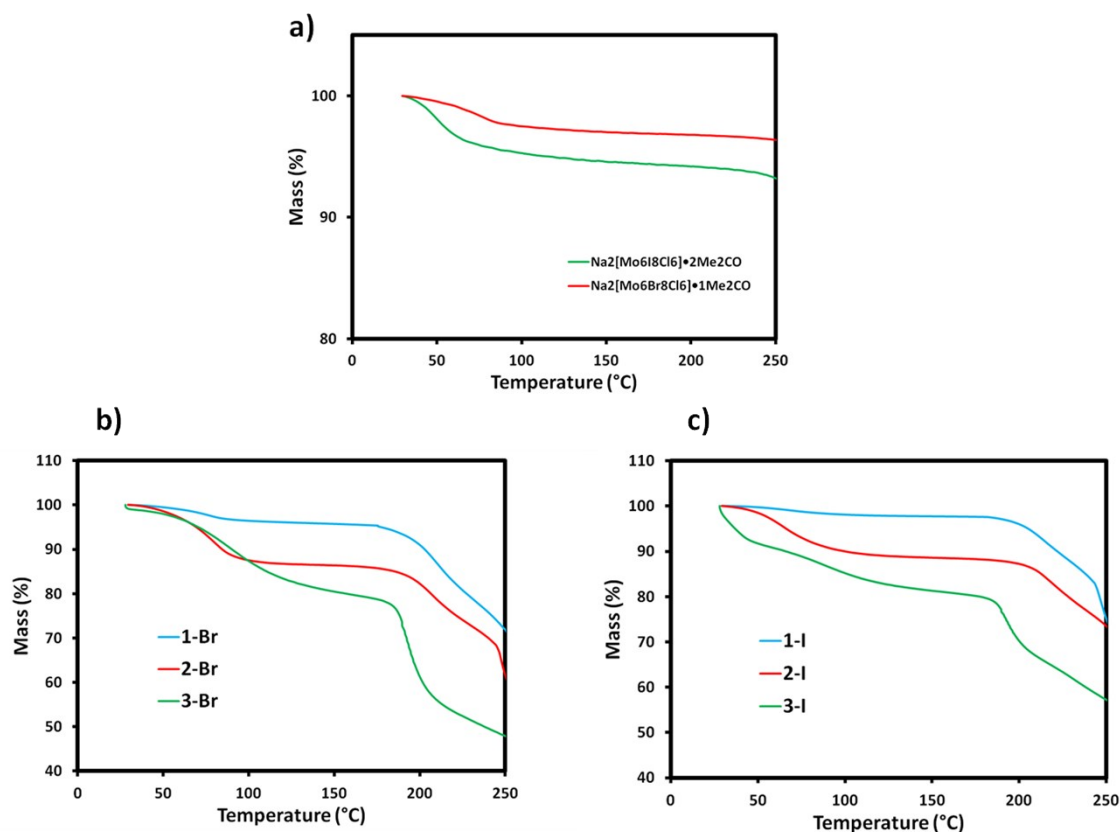


Figure S31: a) Thermogravimetric curves of the water soluble salts of octahedral molybdenum clusters, $\text{Na}_2[\text{Mo}_6\text{X}_8\text{Cl}_6] \cdot \text{Me}_2\text{CO}$ with $\text{X} = \text{Br}$ or I under air atmosphere ($10^\circ\text{C} \cdot \text{min}^{-1}$). The first weight loss occurs between RT and 100°C , is related to the departure of the solvent molecules (at 150°C obs.: 2.8%, calc.: 3.8% for $\text{Na}_2[\text{Mo}_6\text{Br}_8\text{Cl}_6] \cdot \text{Me}_2\text{CO}$, and obs.: 5.0%, calc.: 5.9% for $\text{Na}_2[\text{Mo}_6\text{I}_8\text{Cl}_6] \cdot 2\text{Me}_2\text{CO}$). b and c) Thermogravimetric curves of the supramolecular assemblies built from $\{[\text{Mo}_6\text{Br}_8\text{Cl}_6]@2\text{CD}\}^{2-}$ and $\{[\text{Mo}_6\text{I}_8\text{Cl}_6]@2\text{CD}\}^{2-}$, respectively. This shows the departure free water molecules occur between RT and 150°C . The weight loss observed at 150°C for each compound is reported in the following table.

	1-Br	2-Br	3-Br	1-I	2-I	3-I
calc. (%)	4	13.2	19	3.7	12.4	18
obs. (%)	4.2	13	20	4	11.5	19

The decomposition of the γ -cyclodextrin starts at $180\text{--}200^\circ\text{C}$, involving the collapsing of the supramolecular edifices.

8. Reference

- (1) Dolomanov, O. V.; Bourhis, L. J.; Gildea, R. J.; Howard, J. a. K.; Puschmann, H. OLEX2: A Complete Structure Solution, Refinement and Analysis Program. *J. Appl. Crystallogr.* **2009**, *42* (2), 339–341. <https://doi.org/10.1107/S0021889808042726>.
- (2) Sheldrick, G. M. SHELXT – Integrated Space-Group and Crystal-Structure Determination. *Acta Crystallogr. Sect. Found. Adv.* **2015**, *71* (1), 3–8. <https://doi.org/10.1107/S2053273314026370>.
- (3) Sheldrick, G. M. Crystal Structure Refinement with SHELXL. *Acta Crystallogr. Sect. C Struct. Chem.* **2015**, *71* (1), 3–8. <https://doi.org/10.1107/S2053229614024218>.
- (4) Vorotnikova, N. A.; Vorotnikov, Y. A.; Novozhilov, I. N.; Syrokvashin, M. M.; Nadolinny, V. A.; Kuratieva, N. V.; Benoit, D. M.; Mironov, Y. V.; Walton, R. I.; Clarkson, G. J.; et al. 23-Electron Octahedral Molybdenum Cluster Complex $[\{\text{Mo}_6\text{I}_8\}\text{Cl}_6]^-$. *Inorg. Chem.* **2018**, *57* (2), 811–820. <https://doi.org/10.1021/acs.inorgchem.7b02760>.
- (5) Allouche, L.; Gérardin, C.; Loiseau, T.; Férey, G.; Taulelle, F. Al₃₀: A Giant Aluminum Polycation. *Angew. Chem. Int. Ed.* **2000**, *39* (3), 511–514. [https://doi.org/10.1002/\(SICI\)1521-3773\(20000204\)39:3<511::AID-ANIE511>3.0.CO;2-N](https://doi.org/10.1002/(SICI)1521-3773(20000204)39:3<511::AID-ANIE511>3.0.CO;2-N).
- (6) Assaf, K. I.; Ural, M. S.; Pan, F.; Georgiev, T.; Simova, S.; Rissanen, K.; Gabel, D.; Nau, W. M. Water Structure Recovery in Chaotropic Anion Recognition: High-Affinity Binding of Dodecaborate Clusters to γ -Cyclodextrin. *Angew. Chem. Int. Ed.* **2015**, *54* (23), 6852–6856. <https://doi.org/10.1002/anie.201412485>.
- (7) Ivanov, A. A.; Falaise, C.; Abramov, P. A.; Shestopalov, M. A.; Kirakci, K.; Lang, K.; Moussawi, M. A.; Sokolov, M. N.; Naumov, N. G.; Floquet, S.; et al. Host–Guest Binding Hierarchy within Redox- and Luminescence-Responsive Supramolecular Self-Assembly Based on Chalcogenide Clusters and γ -Cyclodextrin. *Chem. – Eur. J.* **2018**, *24* (51), 13467–13478. <https://doi.org/10.1002/chem.201802102>.